

Paramagnetic Meissner effect analyzed by second harmonics of the magnetic susceptibility: Consistency with a ground state carrying spontaneous currents

Ch. Heinzel, Th. Theilig, and P. Ziemann

Fakultät für Physik, Universität Konstanz, D-78464 Konstanz, Federal Republic of Germany

(Received 28 December 1992; revised manuscript received 15 March 1993)

It has been reported recently by Braunisch *et al.* [Phys. Rev. Lett. **68**, 1908 (1992)] that some ceramic high- T_c superconductors (HTSC's) exhibit a paramagnetic signal if cooled through the superconducting transition temperature in small external magnetic dc fields ($H_{dc} < 1$ Oe). In the present work, this paramagnetic Meissner effect (PME) is experimentally confirmed and further experimental details are reported on this phenomenon. This is accomplished by applying a recently developed compensation technique based on the measurement of the second harmonic of the magnetic ac susceptibility in external dc fields. This technique allows one to detect sensitively the dc magnetization of a HTSC sample and makes it possible to observe the PME under conditions where its dc superconducting-quantum-interference-device signal is totally masked by the dominating diamagnetic behavior of most of the sample. The experiments were performed on melt processed $\text{Bi}_2\text{Sr}_2\text{CaCu}_2\text{O}_{8-x}$ samples, some of which did not exhibit the PME. Thus, a comparison was possible between samples with and without the PME, subjected to different field-cooling procedures. The experimental results are consistent with the occurrence of a reversible transition into a PME state carrying spontaneous orbital currents resulting in corresponding paramagnetic moments, which can be reversibly aligned by small external dc fields. This PME state is attributed to loops containing relatively strong weak links, which are able to remain superconducting close to the bulk T_c of the grains (e.g., at $T/T_c = 0.9$) and in external dc fields of at least 30 Oe.

I. INTRODUCTION

If a superconductor is cooled below its transition temperature T_c in a small external dc field $H_{dc} \leq H_{c1}$ (assuming a type-II superconductor with lower critical field H_{c1}), it is expected to exhibit a diamagnetic response by expelling magnetic flux from the interior of the sample. Under ideal conditions without pinning, this well-known Meissner effect (DME) leads to a bulk susceptibility of $\chi = -1/4\pi$ in gaussian units. If pinning of magnetic flux is possible, the Meissner effect will be incomplete ($|\chi| < 1/4\pi$) but still diamagnetic. In this case, the magnetic behavior becomes hysteretic and the value of the temperature-dependent magnetization depends on whether the sample is field cooled (FC) as above or zero field cooled (ZFC), where the magnetic field is switched on at $T < T_c$ thereby inducing a shielding response of the superconductor. For granular superconductors consisting of superconducting grains which are coupled to each other via weak links, the situation is more complex as intragranular and intergranular effects must be distinguished when discussing the magnetic response. Since bulk samples of the new high- T_c superconductors (HTSC) obtained by sintering are prototypes of granular systems, their magnetic behavior has been extensively studied during the last few years. The experimental results, though revealing quite complicated features in detail due to the interplay between the grains and the weak link network, showed the expected usual diamagnetic response in all cases at least for fields $H_{dc} \geq 1$ Oe. A recent review of this situation can be found in Ref. 1.

Thus it came as a surprise when Braunisch *et al.*² re-

ported on a paramagnetic response of some sintered high- T_c $\text{Bi}_2\text{Sr}_2\text{CaCu}_2\text{O}_{8-x}$ samples during field cooling in small fields $H_{dc} < 1$ Oe. The paramagnetic effect was found to be temperature and time independent well below T_c , similar to the DME, and therefore was addressed as paramagnetic Meissner effect (PME) by these authors. In the following, we will adopt this nomenclature.

Since the absolute value of the paramagnetic magnetization turns out to be small, making the use of superconducting quantum interference device (SQUID) magnetometers necessary for its detection and furthermore the PME is easily masked by the diamagnetic response observed for $H_{dc} \geq 0.5$ Oe, a necessary reaction of an experimentalist is to look for possible artifacts caused by a specific apparatus. But meanwhile, by exchanging samples between different laboratories, such a possibility can be clearly excluded. A summary of the experimental situation in this respect is given in Ref. 3. Thus emphasis must be put on the question as to the physics behind the PME. Two different approaches are possible. One could try to attribute the effect to an interplay between the magnetic response of the grains and that of the weak link network taking into account a distribution of coupling strengths within the network and additionally assuming an inhomogeneous spatial distribution of these couplings. Such an approach is certainly triggered by earlier reports on paramagnetic responses of conventional superconductors. In this context, very early measurements by Steiner and Schoeneck⁴ and Meissner, Schmeisser, and Meissner⁵ have to be mentioned; they found a paramagnetic response of current carrying type-I superconductors in an external magnetic dc field parallel to the current, if the

current was high enough to lead to the intermediate magnetic state. Similar results have been reported for current carrying type-II superconductors and are totally understood on the basis of a conventional theory assuming force-free configurations of the magnetic flux.⁶ Though the above conditions are certainly not given for the PME results reported for high- T_c materials, the measurements may serve as an example that the complicated interplay of different magnetic fields can lead to a counterintuitive magnetic response of a superconducting system.

Another well-documented paramagnetic response is the so-called “differential paramagnetic effect” (DPE), which is observed in ac-susceptibility experiments if type-I or -II superconductors are brought into the intermediate or mixed state by applying an appropriate external dc field H_{dc} .^{7,8} If the DPE is to be observable, the magnetic response of the superconductor should show no hysteresis,⁷ since then the magnetization M is a single-valued function of the field H and a paramagnetic ac susceptibility $\chi = dM/dH$ is reflecting the positive slope of the M vs H curve in the intermediate or mixed state. Thus this effect has been used to distinguish the reversible from the irreversible magnetic regime also in HTSC’s.⁹ The DPE may be important in the present context of the PME, since it is conceivable that the conventional diamagnetic Meissner effect of the grains could induce a differential paramagnetic effect in the weak link network under appropriate conditions.

The second more intriguing approach to explaining the PME is to invoke a new type of ground state for a loop containing a weak link. At the corresponding transition temperature, such a ground state must build up a spontaneous current resulting in a magnetic moment. In an ensemble of loops, these spontaneous currents average out and no net magnetization is expected unless the transition occurs in an external dc field, which should polarize the magnetic moments. Theories predicting such a behavior have been developed prior to the experimental finding of the PME and are mostly based on the assumption of an additional phase shift by π within a weak link (“ π junction”).^{10,11} Quite recently, such a phase shift has been shown to result in a weak link loop of a d -wave superconductor.¹² In this case, the existence of the PME in HTSC samples could be taken as a hint to d -wave pairing in this class of materials.

Another explanation of paramagnetic orbital moments is given by theories dealing with anyon superconductivity.¹³ But experimentally, no convincing evidence for the corresponding internal fields could be provided.¹⁴ Furthermore, since in HTSC ceramics the PME can be suppressed by grinding,³ i.e., by destroying the intergrain couplings, theories based on superconducting loops containing a weak link appear to be a more appropriate approach for explaining this phenomenon.

From these remarks it is quite clear that additional experiments are needed to distinguish between the two above approaches or at least help to let one interpretation appear more probable than the other. It is the aim of our work to present such a contribution mostly based on the behavior of the second harmonics of the magnetic susceptibility of HTSC $\text{Bi}_2\text{Sr}_2\text{CaCu}_2\text{O}_{8-x}$ ceramics, which un-

derwent different cooling procedures in external dc fields. By comparing samples with and without a PME, this effect could be characterized in detail.

The modulus of the complex second harmonic $|\chi_2|$ is especially suited for such a study for the following reasons. If a weak link network is exposed to an external dc field, a large $|\chi_2|$ signal can be observed, which is extremely sensitive to the value of H_{dc} .^{15,16} Furthermore, it has been demonstrated recently¹⁷ that $|\chi_2|$ can be used to sensitively monitor an internal dc field such as the magnetic remanence after field-cooling HTSC ceramics and switching off the external field. Since most of our conclusions are based on this technique, in the following section, II, we will first describe and exemplify its potential by using a HTSC $\text{YBa}_2\text{Cu}_3\text{O}_7$ ceramic, which did not show the PME. Then, in Sec. III the results on the PME of HTSC $\text{Bi}_2\text{Sr}_2\text{CaCu}_2\text{O}_{8-x}$ samples will be presented and discussed.

II. POTENTIAL OF A SECOND-HARMONICS ANALYSIS FOR DETECTING INTERNAL dc FIELDS

If the full cycle of the time-dependent magnetization $M(t)$ covered in an ac-susceptibility measurement using an external field $H(t) = H_{ac} \sin(2\pi ft)$ with frequency f is of odd symmetry with respect to $H = 0$, no even harmonics can be generated.¹⁸ Thus, to obtain especially second harmonics the above point symmetry must be broken. Generally, this can be realized by applying an additional dc field. In more specialized cases, the above symmetry can be broken, e.g., by a spontaneous magnetization or by the preparation of a remanence. Based on these general principles, the generation of higher harmonics in sintered HTSC samples has been extensively studied both experimentally as well as theoretically and a recent review of the field is given by Ishida *et al.*¹⁵

In the context of the present paper, the recently found “memory” effect of the second harmonic¹⁷ is of utmost importance. It means that $|\chi_2| \neq 0$ even for $H_{dc} = 0$ due to the preparation of a remanent magnetization within the sample. Due to the presence of pinning, such a remanence can be easily prepared in HTSC samples by, e.g., field cooling to $T < T_c$ and switching off the external field. The resulting dc remanence $|\mathbf{M}_{rem}| \equiv M_{rem}$ can be further analyzed by applying a special compensation technique using the second harmonic as null detector. To accomplish this, an additional external field \mathbf{H}_{dc} is applied at $T < T_c$. If the direction of \mathbf{H}_{dc} is identical to that during the FC procedure, the induced shielding currents will reduce the remanence and as a consequence, also $|\chi_2|$ is decreasing until at a well-defined field $\mathbf{H}_{dc} = \mathbf{H}_{comp}$ the signal of the second harmonic is minimized. Depending on the linearity of the detection circuitry the minimum can be practically made zero. By performing the same compensation procedure within a SQUID magnetometer, it could be independently demonstrated that the magnetization induced by \mathbf{H}_{comp} compensates the remanence. For fields \mathbf{H}_{dc} larger or smaller than \mathbf{H}_{comp} one has an overcompensated or undercompensated state with a

nonzero value of χ_2 . Furthermore, as has been shown in Ref. 17, H_{comp} is proportional to M_{rem} and can be used to determine M_{rem} quantitatively.

The above-described compensation technique is demonstrated in Fig. 1 for a sintered $\text{YBa}_2\text{Cu}_3\text{O}_7$ sample (size $2 \times 1 \times 5 \text{ mm}^3$, $T_c = 90.1 \text{ K}$), which was field cooled to 77 K in $H_{\text{dc}} = 30 \text{ Oe}$. The sample is positioned at the center of a pair of Helmholtz coils providing the external exciting ac field (frequency $f = 1049 \text{ Hz}$). The magnetic response of the sample is detected by a pair of counter-wise wound pick-up coils and measured by a vector-lock-in amplifier tuned to $2f$. The amplitude of the ac field H_{ac} is 1 Oe in this case. Additional dc fields up to $H_{\text{dc}} = 110 \text{ Oe}$ can be superposed via the same Helmholtz coils. The sample is thermally coupled to a liquid-nitrogen bath and its temperature can be varied and controlled between 65 and 300 K . More details on the susceptometer can be found in Ref. 19. In Fig. 1(a), the compensated state is approached by reducing the field, which was applied during FC (cf. arrows). The minimum of the second harmonic (here given by the corresponding voltage) at H_{comp} can clearly be seen. It is important to note that after reversing the field direction ($H_{\text{dc}} < 0$) no minimum is obtained for increasing field values. In the following we adopt the convention that positive compensation fields $H_{\text{comp}} > 0$ always compensate internal mag-

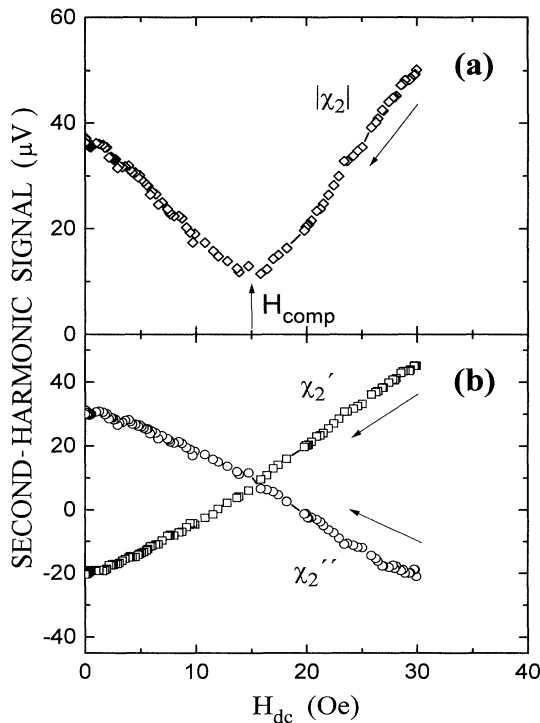


FIG. 1. Second harmonic of the magnetic ac susceptibility ($H_{\text{ac}} = 1 \text{ Oe}$) obtained for a $\text{YBa}_2\text{Cu}_3\text{O}_7$ ceramic after field cooling in a dc field of $H_{\text{dc}} = 30 \text{ Oe}$ and stepwise reducing H_{dc} . (a) Modulus $|\chi_2|$ of the complex second harmonic. (b) Real (χ_2') and imaginary (χ_2'') parts of the second harmonic. Additional experimental details are given in the text.

netizations, which were produced by external fields parallel to H_{comp} . Thus from Fig. 1(a) one can immediately conclude that a paramagnetic remanence has been compensated at H_{comp} as is expected for the FC remanence in a type-II superconductor with pinning. To corroborate that the sample at H_{comp} is really in a compensated state, in Fig. 1(b) the real (χ_2') and imaginary (χ_2'') parts of the second harmonic are presented. Here, the important feature is the intersection of the real and the imaginary part at H_{comp} . The finite values of χ_2' and χ_2'' at H_{comp} are due to the experimental imperfection of the electrical circuitry (under ideal conditions $|\chi_2| = 0$ at H_{comp}). Taking this into account, the observed intersection of χ_2' and χ_2'' indicates a change of sign of both of these quantities. For a virgin sample such a change of sign is only expected at $H_{\text{dc}} = 0 \text{ Oe}$.^{15,20} Thus at H_{comp} one has the effective zero point for dc fields in accordance with the idea of compensation.

After this example, the interpretation of the following results obtained after zero field cooling the same $\text{YBa}_2\text{Cu}_3\text{O}_7$ sample, which are shown in Fig. 2, is straightforward. Starting with a virgin sample from $H_{\text{dc}} = 0 \text{ Oe}$ no compensation can be expected for increasing fields [$H_{\text{dc}} < 50 \text{ Oe}$, solid squares in Fig. 2(a)]. Only

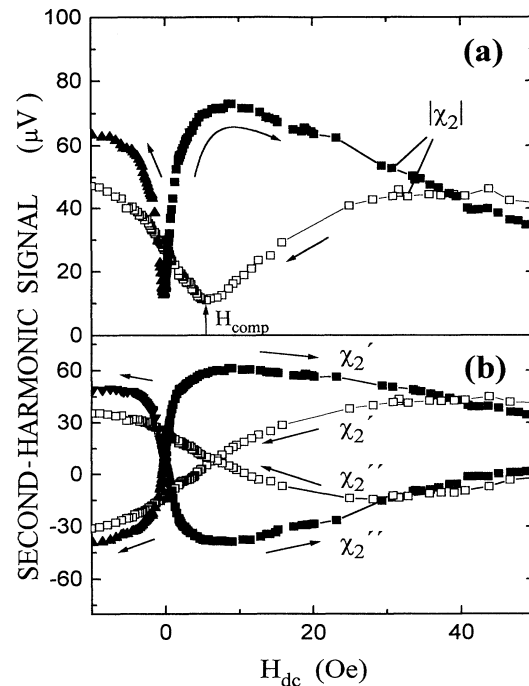


FIG. 2. Second harmonic of the magnetic ac susceptibility ($H_{\text{ac}} = 2 \text{ Oe}$) obtained for a $\text{YBa}_2\text{Cu}_3\text{O}_7$ ceramic (same as in Fig. 1) after zero field cooling (ZFC) to $T = 77 \text{ K}$. (a) Modulus $|\chi_2|$ of the complex second harmonic for increasing dc fields (solid squares) up to 50 Oe . The open squares are obtained by reducing H_{dc} from 50 Oe . An additional ZFC experiment, with the direction of H_{dc} reversed, delivers the solid triangles. (b) Real (χ_2') and imaginary (χ_2'') parts corresponding to the procedure described in (a). The symbols used in (a) and (b) correspond to each other; the field changes are indicated by arrows.

after decreasing the field again [open squares in Fig. 2(a)], is a remanent magnetization developed, which can be compensated at H_{comp} . Alternatively, this remanence becomes visible by the finite signal at $H_{\text{dc}}=0$ Oe after decreasing the field. Correspondingly, sign changes of χ'_2 and χ''_2 are expected at $H_{\text{dc}}=0$ Oe for increasing fields and at H_{comp} for decreasing fields. This is exactly confirmed by the experiments shown in Fig. 2(b) (the solid triangles in Fig. 2 were obtained by an additional ZFC experiment with a reversed direction of H_{dc}).

Another point should be noted. The remanent magnetization is a consequence of the hysteretic behavior of the sample, which manifests itself by the different branches in Fig. 2(a) obtained for increasing and decreasing fields, respectively. In other words, this type of measurement allows one to determine the reversible and the irreversible regimes of the magnetic behavior of a HTSC sample. We close this section by summarizing the most important properties of our second-harmonics technique.

(1) H_{comp} is a measure of the value of the internal dc magnetization.

(2) At H_{comp} a sign change occurs for both χ'_2 and χ''_2 (after subtracting the finite value $|\chi_2|$ at H_{comp}).

(3) If $H_{\text{comp}} > 0$, the internal magnetization is paramagnetic in hysteretic samples. In any case, the internal magnetization is parallel to the external compensation field.

(4) Irreversible behavior is reflected by two different $|\chi_2|$ branches for increasing and decreasing dc fields, respectively.

We will rely on these properties when interpreting the following PME results.

III. THE PARAMAGNETIC MEISSNER EFFECT

A. dc (SQUID) measurements

The samples studied in this work were all of the $\text{Bi}_2\text{Sr}_2\text{CaCu}_2\text{O}_{8-x}$ type, prepared by a melt cast procedure. The details of the preparation as well as the results of an extended series of measurements characterizing the different samples will be described in Ref. 3. Here, we quote only the most important results: no magnetic contaminations were detected within the resolution of some ppm and the 2:2:1:2 stoichiometry was confirmed within 10–15%. No significant chemical differences could be found between samples with and without a PME.

The dc-magnetization measurements were performed in a specially designed SQUID magnetometer. Here, the sample is mounted onto a sapphire lever and held fixed in the center of a pair of superconducting Helmholtz coils. The signal is obtained through a pair of counterwound superconducting pick-up coils, which are glued onto another sapphire part closely above (~ 1 mm) the sample. Thus the sample and the pick-up coils are not moved during the measurement. The superconducting leads are connected to a commercial rf SQUID. By thermally decoupling the sample holder from the Helmholtz and pick-up coils, the magnetization can be measured between 5 and 120 K. The system is magneti-

cally shielded by mumetal and a superconducting Nb cylinder. Nevertheless, additional experiments showed that the Earth's magnetic field could not totally be shielded. Thus FC experiments in nominal fields as applied in the Helmholtz coils below 0.1 Oe are not well defined with respect to the value of H_{dc} .

The results of magnetization measurements performed on a sample exhibiting the PME are shown in Fig. 3. Here, the number of flux quanta ($\phi_0 = h/2e$) as monitored by the SQUID is plotted versus the temperature during FC procedures in different external dc fields as assigned to each curve. To obtain the magnetization in gaussian units, the SQUID signal must be multiplied by the factor $2.38 \times 10^{-3} \text{ G}/\phi_0$. The PME can clearly be observed for nominal fields $H_{\text{dc}} \leq 0.17$ Oe. For larger external fields the signals become diamagnetic (note the different scale for the fields 0.44 and 1.05 Oe in Fig. 3). As a characteristic feature, the PME is always preceded by a small but significant diamagnetic response starting at $T = T_c$. Another point is important. In Fig. 3, the signal height of the PME appears to be independent of the nominal value of H_{dc} . But this result is probably due to the incomplete shielding of the Earth's magnetic field as mentioned above. This assumption is supported by looking at the dc susceptibility $\chi_{\text{dc}}^s = M_s/H_{\text{dc}}$ (M_s is the constant magnetization at $T \ll T_c$ measured in gaussian units). In the inset of Fig. 3, χ_{dc}^s is given for different external fields H_{dc} . The solid line is a fit to $\chi_{\text{dc}}^s = \chi_0 + m/(H_{\text{dc}} + H_0)$ resulting in $\chi_0 = -0.012/4\pi$ (expressed relative to the shielding behavior as determined by ZFC, one obtains $\chi_0 = 14.1\%$), $H_0 = 0.1$ Oe, and $m = 0.005 \text{ G}/4\pi$. These numerical values are in

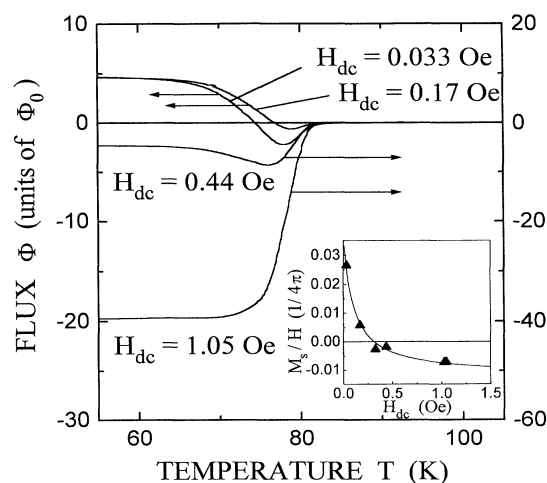


FIG. 3. Temperature dependence of the dc magnetization of a $\text{Bi}_2\text{Sr}_2\text{CaCu}_2\text{O}_{8-x}$ ceramic cooled in dc fields as assigned to each curve (note the different scales for M as indicated by the horizontal arrows). The solid lines result from the high density of data points (ten points per kelvin) obtained from the SQUID in units of flux quanta ϕ_0 . The inset shows the saturation susceptibility at $T \ll T_c = 83$ K as a function of the applied dc field. The solid line is a fit of the expression given in the text to the data.

close agreement with those reported by Braunisch *et al.*,^{2,3} thus providing an independent confirmation of the PME. The fact that the experimental data can be described by the above expression for χ_{dc}^s means that for fields $H_{dc} \ll H_0$ a constant value of χ_{dc}^s is obtained resulting in a linear decrease of the PME magnetization of the form $M_s = (m/H_0)H_{dc}$. On the other hand, for $H_{dc} > H_0 = 0.1$ Oe the expression for χ_{dc}^s leads to a field-independent PME magnetization.

There is another noteworthy point resulting from the above fit to the data. At $H_{dc} \geq 1$ Oe no direct indication for a PME can experimentally be detected. Nevertheless, χ_{dc}^s found for, e.g., $H_{dc} = 1$ Oe, is still significantly above the extrapolated saturation of the DME as given by χ_0 . We conclude that a field-independent PME may be present up to rather high fields (in the following we will present evidence for its presence at $H_{dc} = 10$ Oe), but cannot be resolved by dc measurements due to the large diamagnetic signals. On the other hand, if the PME is related to weak links as it is deduced from the grinding experiments mentioned in the Introduction, its possible presence at 10 Oe implies rather high coupling strengths.

While the DME as observed during FC in fields $H_{dc} > 1$ Oe is mostly governed by the DME of the individual grains, insight into the magnetic response of the weak link network can be obtained by ZFC experiments, which monitor the shielding behavior. This becomes clear by referring to theoretical results on two-dimensional Josephson networks²³ with pointlike grains interconnected to the nearest neighbors via identical weak links. Such a network shows the expected shielding behavior in ZFC experiments, but does not exhibit a DME. This is in accordance with the fact that the magnetic flux through a non-simply-connected superconductor is conserved. Corresponding ZFC results for a PME sample are shown in Fig. 4, where χ_{dc} is plotted as a function of temperature for two different fields H_{dc} (0.17 Oe,

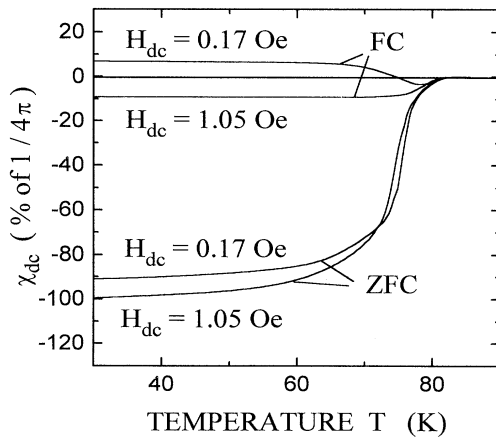


FIG. 4. Temperature dependence of the dc susceptibility of a $\text{Bi}_2\text{Sr}_2\text{CaCu}_2\text{O}_{8-x}$ ceramic (same as in Fig. 3) obtained by field-cooled (FC) or zero-field-cooled (ZFC) experiments in fields as assigned to each curve. The solid lines result from the high density of data points (cf. Fig. 3).

1.05 Oe) observed during FC and ZFC procedures. Here, the steep increase of χ_{dc} at $T = 75$ K in the ZFC experiment can be attributed to the decoupling of the weak link network in analogy to ac-susceptibility measurements, where this decoupling of grains can be studied by applying additional decoupling dc fields.^{21,22} In the present case, Fig. 4 shows that a field of $H_{dc} = 1$ Oe has practically no influence on the shielding behavior of the network though it is sufficient to totally mask the PME during FC. The insensitivity of the shielding behavior is corroborated by corresponding ac-susceptibility measurements for this sample. The temperature dependence of the real part $\chi'(T)$ measured by applying an ac field of $H_{ac} = 0.05$ Oe is not influenced by an additional dc field of $H_{dc} = 1$ Oe. More details on the ac-susceptibility measurements will be given in the following section.

B. Fundamental ac susceptibility

In the following, we concentrate on two samples, one of which is exhibiting the PME (sample 1 corresponding to KaMu96 in Ref. 3), for the other (sample 2 corresponding to Bo105b in Ref. 3) no PME could be detected. In Fig. 5, the temperature dependences of the real (χ') and the imaginary (χ'') part of the fundamental ac susceptibility for these two samples are presented. Since their transition temperatures T_c are different as given in the figure caption, the temperature is expressed in re-

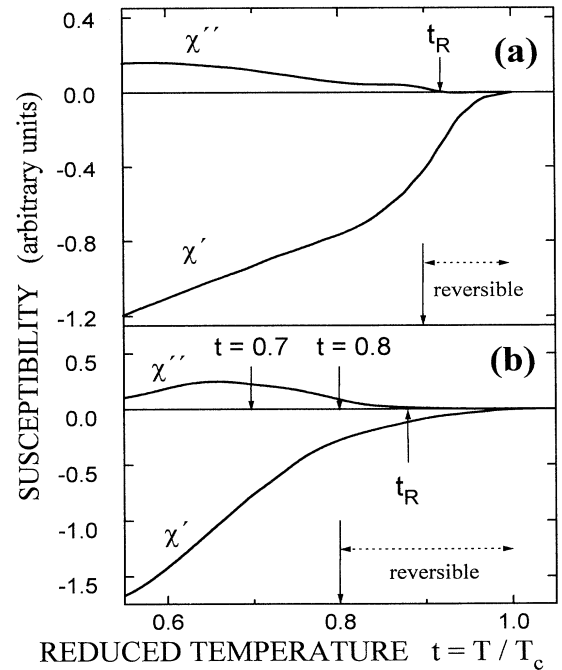


FIG. 5. Temperature dependence of the real (χ') and imaginary (χ'') parts of the fundamental ac susceptibility [$f = 1049$ Hz, $H_{ac} = 2$ Oe in (a) and 0.05 Oe in (b)] for two different $\text{Bi}_2\text{Sr}_2\text{CaCu}_2\text{O}_{8-x}$ samples. (a) Sample 2 ($T_c = 86.8$ K), without PME. (b) Sample 1 ($T_c = 73.8$ K), with PME. The dashed horizontal arrows indicate the temperature range, where a reversible magnetic behavior is observed by the second harmonics.

duced units $t = T/T_c$. For both samples, a temperature range can be found with $t_R \leq t \leq 1.0$, where significant shielding occurs as indicated by the negative value of χ' , while the corresponding imaginary part χ'' is zero within the experimental resolution. For an ideal ceramic superconductor containing perfect grains, such a behavior is expected if the grains are still decoupled from each other at T close to T_c and their size is of the order of the London penetration length λ . In this case, the temperature dependence of χ' for $t \geq t_R$ is due to the corresponding dependence of λ . In the more realistic case, the grains, though not perfectly free of weak links, must be small enough that intragranular losses are not observable by the applied ac technique. For temperatures $t < t_R$, the superconducting coupling between grains sets in, leading to a much stronger shielding response which now is accompanied by intergranular losses as indicated by the nonzero imaginary parts. This overall behavior of the ac susceptibility is quite common for HTSC ceramics^{21,22} and the above interpretation is widely accepted.¹ The imaginary part of sample 2 in Fig. 5(a) shows a double-peak structure, which may be taken as a hint that the weak link network is more inhomogeneous than in sample 1 [Fig. 5(b)] and may consist of two subnetworks with different average coupling strengths. But the general behavior of both samples is quite similar and no specific signature of a PME can be extracted from the fundamental ac susceptibility. This is contrasted by the following analysis of the second harmonic which is performed for both samples at the different reduced temperatures as indicated in Fig. 5(b) by arrows. These measurements additionally reveal the temperature range, where the magnetic response of the samples behaves reversibly as judged from the second harmonic. The result is also indicated in Fig. 5.

C. Analysis of the second harmonics

In the following we present the results of the second-harmonics analysis as described in Sec. II. If not otherwise stated the samples are cooled to a specific reduced temperature in the Earth's magnetic field, which in our case amounts to 0.1 Oe as separately determined. Then the external dc field is applied and the real (χ'_2) and imaginary (χ''_2) parts of the second harmonic are determined for increasing fields followed by the corresponding measurements for decreasing fields. In Fig. 6 the data taken at $t = 0.9$ are shown for sample 2, which does not exhibit a PME. Here, the results for increasing H_{dc} are given by closed symbols, those for decreasing fields by open symbols. The observed overall behavior of $|\chi_2|$ as given in Fig. 6(a) is typical of ceramic HTSC samples after ZFC with a steep increase of the signal for small external fields followed by a broad decrease for larger H_{dc} values. Theoretically, a possible explanation is to assume a weak link network, where the maximum current through a weak link I_c depends on the local magnetic field H_{loc} in a Kim-like manner, i.e., $I_c \sim (H_{loc} + H_0)^{-1}$.²³ The more remarkable feature of the data in Fig. 6 is the observed reversibility. On the other hand, this fits very nicely with the behavior of the fundamental ac susceptibility ob-

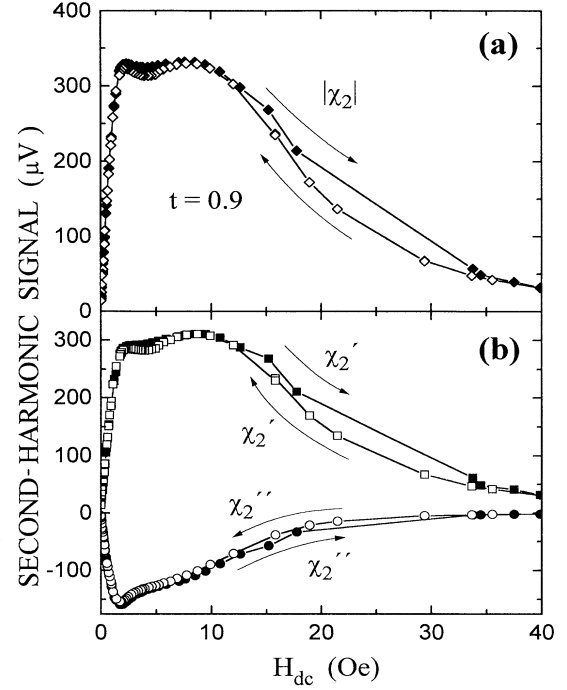


FIG. 6. Second harmonic of the magnetic ac susceptibility ($H_{ac} = 2$ Oe) obtained for sample 2 (no PME) after field cooling in the Earth's magnetic field to a reduced temperature of $t = 0.9$. (a) $|\chi_2|$ of the complex second harmonic for increasing fields are given by solid symbols. (b) Real (χ'_2) and imaginary (χ''_2) parts corresponding to (a).

tained for this sample at the same temperature $t = 0.9$. Here, no ac losses could be resolved as indicated by the vanishing imaginary part χ'' [cf. Fig. 5(a)]. Another point is important. For the above sample without a PME, only at $H_{dc} = 0$ Oe is a sign change of both χ'_2 and χ''_2 found. Thus, following the rules stated in Sec. II, it is concluded that there is no dc magnetization of the sample, which could be compensated by applying a field H_{dc} , i.e., $H_{comp} = 0$ Oe. It further should be noted that the curves of Fig. 6 show an even symmetry with respect to reversing the direction of the external dc field.

The corresponding results are quite different for sample 1, which exhibits a PME. This is demonstrated in Fig. 7, where data taken at $t = 0.8$ are presented. As for the sample without the PME a remarkable reversibility of the second harmonic for increasing and decreasing dc fields is observed at this temperature. But the most important new feature in Fig. 7 is the steep decrease of $|\chi_2|$ at $H_{comp} = 2.9$ Oe. At this finite external field both the real and the imaginary part of the second harmonic change their sign as shown in Fig. 7(b). In accordance with the rules given in Sec. II, this is clear evidence that by applying H_{comp} a dc magnetization is compensated. Since such a reversible behavior with a finite compensation field H_{comp} is observed only for samples exhibiting the PME, we attribute the magnetization, which is necessary to observe $H_{comp} \neq 0$ to the PME. Furthermore,

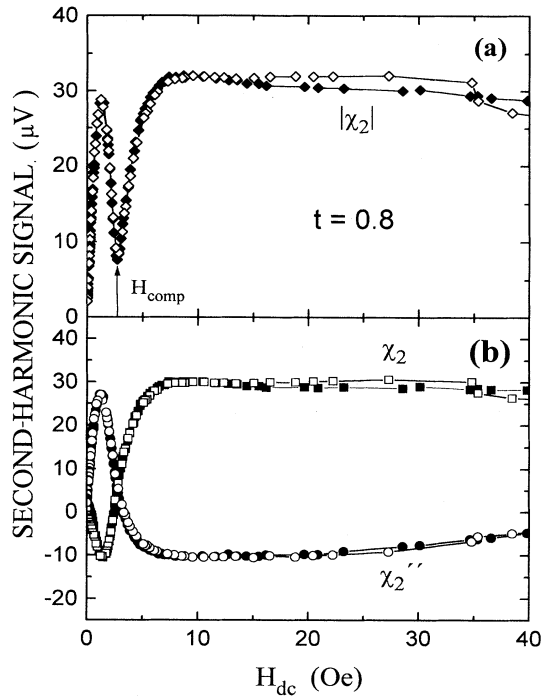


FIG. 7. Second harmonic of the magnetic ac susceptibility ($H_{ac}=2$ Oe) for sample 1 (with PME) after field cooling in the Earth's magnetic field to a reduced temperature of $t=0.8$. (a) $|\chi_2|$ for increasing fields are given by solid symbols, for decreasing fields by open symbols. The compensation minimum at H_{comp} is indicated by an arrow. (b) Real (χ_2') and imaginary (χ_2'') parts corresponding to (a).

since as has been mentioned in Sec. II, the value of H_{comp} is a direct measure of the magnetization, the reversibility found can be interpreted in the following way. The PME is definitely not destroyed in external fields up to $H_{dc}=10$ Oe as the effect of its overcompensation by H_{dc} is still clearly visible. For even larger fields the data do not allow such a conclusion, but if the PME is destroyed by these large fields, it obviously can be reversibly restored by decreasing the field. It is noteworthy that identical values for H_{comp} are obtained for decreasing and increasing fields H_{dc} leading to the conclusion that the corresponding PME magnetizations are identical. In this context, another feature not shown in Fig. 7 is of utmost importance. All curves of Fig. 7 exhibit an even symmetry with respect to a reversal of the field direction. In accordance with Sec. II, one concludes that the magnetization due to the PME can be reversed by reversing the external magnetic field. Even more specific, this reversal is complete since the value of H_{comp} is independent of the direction of H_{dc} . Thus the results of the second harmonics suggest the astonishing picture of magnetic moments due to the PME, which are saturated even in extremely small fields of the order of $H_0=0.1$ Oe and which reversibly adjust to the direction of the external dc field. Of course, such a reversible response of the PME moments is also expected for the exciting ac fields. Consequently, no losses are observed in the corresponding fundamental ac

susceptibility (cf. Fig. 5). In the second-harmonic experiment, the exciting field is symmetrically applied relative to H_{dc} . Thus its effect is averaged out as long $H_{ac} \leq H_{comp}$. Only for larger ac amplitudes is a smearing out of the compensation effect expected. This is confirmed by experiment as shown in Fig. 8. Here, $|\chi_2|$ for another sample exhibiting the PME (sample 3 corresponding to KnBock1 in Ref. 3) is shown as a function of the external dc field. The data are taken at $t=0.93$ and again a reversible behavior is found. In Fig. 8(a) the standard amplitude $H_{ac}=2$ Oe had been applied leading to the well-resolved signature of the PME at H_{comp} . By increasing the amplitude to $H_{ac}=5$ Oe $> H_{comp}$, the compensation effect is smeared out as can be seen in Fig. 8(b).

The above picture of PME moments suggested by the results of the analysis of the second harmonics is independent of the specific nature of the process producing the moments. But, if weak links are thought responsible for the PME, the following additional qualitative statements can be made. At the high reduced temperatures analyzed so far, only the strongest weak links are still superconducting while most of the network is already decoupled. Thus at these high temperatures it appears plausible to assume clusters of loops within the sample, which contain the strongest weak links. At T_c , these weak links reversibly pass through the transition into the PME state and in external dc fields a corresponding magnetization becomes

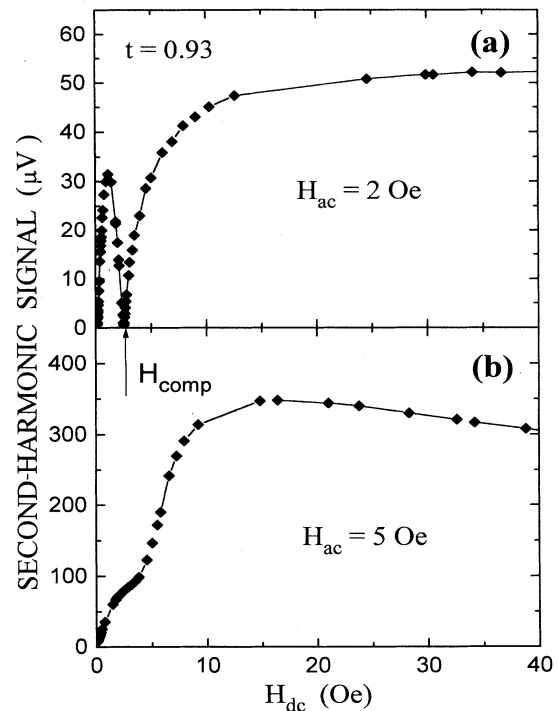


FIG. 8. Influence of the amplitude of the exciting ac field H_{ac} on the second harmonic of the magnetic ac susceptibility of sample 3 (with PME). (a) $H_{ac}=2$ Oe. (b) $H_{ac}=5$ Oe. In both cases, the samples had been cooled to $t=0.93$ in the Earth's magnetic field and the data were taken for increasing dc fields H_{dc} .

measurable. If this picture is qualitatively correct, there should be an upper limit H_{\max} above which the superconductivity even of the strongest weak links involved in the PME will be suppressed. From our previous experience with HTSC ceramics,^{21,22} we expect H_{\max} to be of the order of some tens of oersteds. Thus the reason that the PME can be observed only in extremely small dc fields by the SQUID technique is due to the fact that higher fields produce a large diamagnetic response from the rest of the sample not containing the PME loops. In this context, the following FC experiment is of interest. Here, sample 1 is cooled through the transition temperature T_c in an external field of $H_{dc} = 30$ Oe down to a reduced temperature of $t = 0.88$. Then, during a stepwise reduction of the field, the signal of the second harmonic is determined. The corresponding results are shown in Fig. 9. The most important feature of these data is that they demonstrate the presence of the PME by exhibiting a compensated magnetization at $H_{comp} \neq 0$ even after FC in a relatively high dc field. Furthermore, the value of H_{comp} is found to be identical within our resolution with that obtained after cooling in the Earth's magnetic field. These results provide strong additional support for the idea of a reversible transition into a PME state with magnetic moments, which are saturated even in very small fields.

It is worth noting that the interpretation introduced so far did not rely on any assumption of what subsystem of the sample is causing the necessary nonlinearity to make

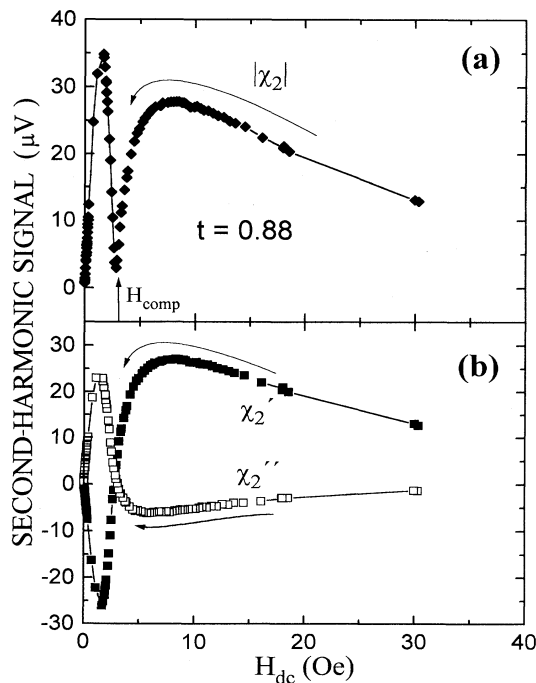


FIG. 9. Second harmonic of the magnetic ac susceptibility ($H_{ac} = 2$ Oe) obtained for sample 1 (with PME) after field cooling to $t = 0.88$ in a field of 30 Oe. The data were taken by stepwise decreasing this external field to zero. (a) Modulus $|\chi_2|$ of the complex second harmonic. (b) Real (χ_2') and imaginary (χ_2'') parts corresponding to (a).

the second harmonics visible. As has been shown for sample 2 (see Fig. 6), second harmonics are also produced in a HTSC ceramic, which does not exhibit the PME. The important point is that the magnetization due to the PME is coupled to the conventionally, i.e., diamagnetically responding part of the sample, which also is producing the second harmonics. The degree of detection of the PME by the above compensation technique can be drastically changed by lowering the temperature. Then, more and more weak links become superconducting and will contribute to the magnetic response of the sample. This increasing coupling of the network by reducing the temperature leads to intergranular losses as can be seen from the imaginary part of the fundamental susceptibility (cf. Fig. 5). For sample 1, these losses have a maximum at $t = 0.65$. For even lower temperatures the shielding ability of the sample is still increasing hindering a small external field from penetrating the sample in a ZFC procedure. In a second-harmonic experiment, losses should show up as irreversibility, i.e., a difference between $|\chi_2|$ for increasing and decreasing external fields. This behavior is demonstrated in Fig. 10, where $|\chi_2|$ of sample 1 is shown for increasing fields (closed symbols) after FC in the Earth's magnetic field to the reduced temperatures

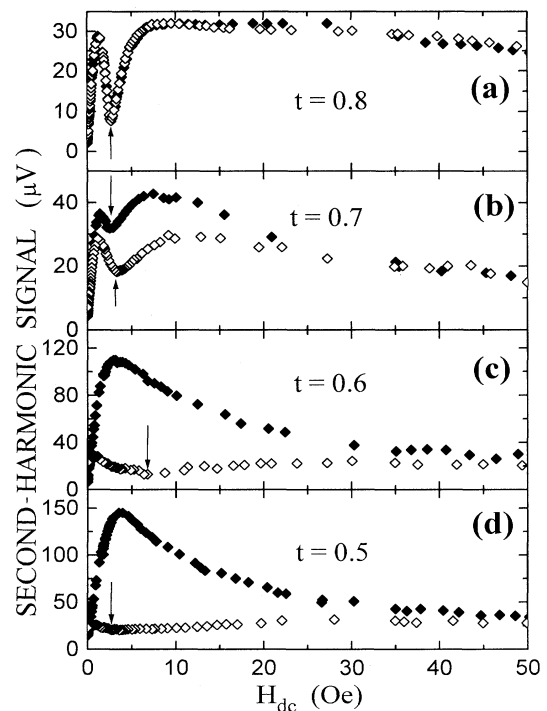


FIG. 10. Modulus $|\chi_2|$ of the complex second harmonic ($H_{ac} = 2$ Oe) obtained for sample 1 (with PME) after field cooling in the Earth's magnetic field to different reduced temperatures as assigned to each figure (a)–(d). The data taken for increasing dc fields (up to $H_{dc} = 100$ Oe) are given by solid symbols, those for decreasing fields by open symbols. The arrows indicate the field values for which an intersection and change of sign of the corresponding real and imaginary parts were observed.

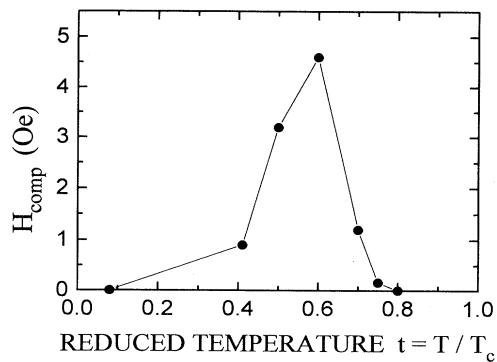


FIG. 11. Temperature dependence of the compensation fields H_{comp} obtained for sample 1. In all cases, the sample is cooled in the Earth's magnetic field to the corresponding reduced temperature and an external field of $H_{\text{dc}} = 100$ Oe is applied. H_{comp} is determined during decreasing H_{dc} and is reflecting the ZFC remanence of the sample.

indicated in Figs. 10(a)–10(d). After a maximum of $H_{\text{dc}} = 100$ Oe, the field is decreased and corresponding $|\chi_2|$ data are recorded (open symbols in Fig. 10). At $t = 0.8$, the behavior is reversible within our resolution and the typical signature of the PME is clearly obtained. At $t = 0.7$, for increasing fields the influence of the PME is still visible [upper arrow in Fig. 10(b)] but strongly reduced. For decreasing fields, hysteretic behavior sets in for $H_{\text{dc}} \leq 20$ Oe and the field necessary to compensate the total internal magnetization is shifted to higher values (the difference ΔH_{comp} for increasing and decreasing fields amounts to 1.2 Oe). This shift is easily attributed to the additional remanent magnetization due to the hysteretic behavior of the weak link network. Further reduction of the temperature to $t = 0.6$ leads to the effect that for increasing fields the PME is now totally masked by the conventional behavior of the main weak link network, though from the complementary SQUID measurements its presence is obvious (cf. Fig. 3). For decreasing fields hysteresis starts at approximately $H_{\text{dc}} \leq 30$ Oe and the observed compensation at $H_{\text{comp}} = 8$ Oe is again governed by the remanent magnetization of the hysteretic network (H_{comp} is determined from the intersection of χ'_2 and χ''_2 not shown in the figure and indicated by an arrow). This interpretation is corroborated by the fact that the curves no longer exhibit an even symmetry with respect to reversing H_{dc} . The results obtained at $t = 0.5$ and lower are qualitatively very similar to those at $t = 0.6$ except that the minimum of $|\chi_2|$ obtained for decreasing fields is shifted to smaller values of H_{comp} . This is in accordance with the above-mentioned enhancement of the shielding ability of the network. Actually, if the H_{comp} values, which are attributed to the remanence of the network, are plotted versus the reduced temperature t , the curve

shown in Fig. 11 is obtained. It nicely reflects the loss peak as obtained from the fundamental ac susceptibility of this sample (cf. Fig. 5). A last point should be emphasized. For both types of samples with and without a PME, a temperature range is observed where the magnetic response is reversible. Thus this reversibility is not necessary for the PME providing evidence against an interpretation in terms of the differential paramagnetic effect, for which a high degree of reversibility is needed as mentioned in the Introduction. Furthermore, for any effect hinging on the interplay between the magnetic response of the grains and the weak link network, we would expect a dependence on the value of the applied dc field in contrast to the experimental results reported above for the PME.

IV. SUMMARY

A new compensation technique has been introduced based on the measurement of the second harmonic of the magnetic susceptibility of ceramic HTSC samples, which allows one to determine their dc magnetization. This technique is applied to further characterize the PME in $\text{Bi}_2\text{Sr}_2\text{CaCu}_2\text{O}_{8-x}$ samples, which showed this effect in dc (SQUID) measurements. Due to its high sensitivity to dc magnetizations, the second-harmonic analysis makes it possible to detect the PME under experimental conditions, where its dc (SQUID) signal is totally masked by the diamagnetic behavior of most of the sample. The results extracted in this way are consistent with the idea of a reversible transition into a PME state carrying orbital currents resulting in corresponding paramagnetic moments, which can be saturated even in extremely small external fields. This PME state is attributed to loops containing relatively strong weak links, which are still superconducting even close to the bulk- T_c value ($t = 0.9$) of the grains. Furthermore, some details found experimentally such as the constant value of H_{comp} for different external fields and cooling procedures, let models appear quite improbable, which rely on a complicated interplay between the intragranular and intergranular magnetic response.

ACKNOWLEDGMENTS

We thank our colleagues from Cologne, W. Braunisch, N. Knauf, J. Bock, and E. Preisler for sample preparation, communication of results prior to publication, and critical discussions. We also have benefited very much from discussions and comments by many other colleagues, especially by Professor W. Buckel, Professor H. Claus, Dr. A. Majhofer, and Dr. Th. Wolf. The financial support by Bundesministerium für Forschung und Technologie (BMFT) and by Land Baden-Württemberg (MWK) is gratefully acknowledged.

¹Magnetic Susceptibility of Superconductors and Other Spin Systems, edited by R. A. Hein, Th. L. Francavilla, and D. H. Liebenberg (Plenum, New York, 1991).

²W. Braunisch, N. Knauf, V. Kataev, S. Neuhausen, A. Grütz,

A. Kock, B. Roden, D. Khomskii, and D. Wohlleben, Phys. Rev. Lett. **68**, 1908 (1992).

³W. Braunisch, N. Knauf, G. Bauer, A. Kock, A. Becker, B. Freitag, A. Grütz, V. Kataev, S. Neuhausen, B. Rhoden, D.

- Khomskii, D. Wohlleben, J. Bock, and E. Preisler, Phys. Rev. B (to be published).
- ⁴K. Steiner and H. Schoeneck, Phys. Z. **44**, 364 (1943).
- ⁵W. Meissner, F. Schmeisser, and H. Meissner, Z. Phys. **130**, 521 (1951); **130**, 529 (1951).
- ⁶M. A. R. LeBlanc, Phys. Rev. **143**, 220 (1966).
- ⁷R. A. Hein and R. L. Falge, Jr., Phys. Rev. **123**, 407 (1961).
- ⁸A. K. Grover, S. Ramakrishnan, R. Kumar, P. L. Paulose, G. Chandra, S. K. Malik, and P. Chaddah, Physica C **192**, 372 (1992).
- ⁹A. F. Khoder, M. Couach, and J. L. Jorda, Phys. Rev. B **42**, 8714 (1990).
- ¹⁰L. N. Bulaevskii, V. V. Kuzii, and A. A. Sobyenin, Zh. Eksp. Teor. Fiz. **25**, 314 (1977) [Sov. Phys. JETP Lett. **25**, 290 (1977)].
- ¹¹B. I. Spivak and S. A. Kivelson, Phys. Rev. B **43**, 3740 (1991).
- ¹²M. Sigrist and T. M. Rice, J. Phys. Soc. Jpn. **61**, 4283 (1992).
- ¹³G. S. Canright and M. D. Johnson, Comments Condens. Matter. Phys. **15**, 77 (1990).
- ¹⁴B. Goss Levi, Phys. Today **44** (2), 17 (1991).
- ¹⁵T. Ishida, R. B. Goldfarb, S. Okayasu, Y. Kazumata, J. Franz, T. Arndt, and W. Schauer, in *High-Temperature Superconductors*, edited by J. J. Pouch, S. A. Alterovitz, and R. R. Romanofsky (TransTech, Aedermannsdorf, Switzerland, 1992).
- ¹⁶C. D. Jeffries, Q. H. Lam, Y. Kim, A. Zettl, and M. P. Klein, Phys. Rev. B **39**, 11 526 (1989).
- ¹⁷Th. Ritzl, Ch. Heinzl, Ch. Neumann, and P. Ziemann, Appl. Phys. Lett. **60**, 2297 (1992).
- ¹⁸L. Ji, H. Sohn, G. C. Spalding, C. J. Lobb, and M. Tinkham, Phys. Rev. B **40**, 10 936 (1989).
- ¹⁹Ch. Neumann, P. Ziemann, J. Geerk, and H. C. Li, J. Less-Common Met. **151**, 363 (1989).
- ²⁰T. Ishida and R. B. Goldfarb, Phys. Rev. B **41**, 8937 (1990).
- ²¹Ch. Heinzl, Ch. Neumann, P. Ziemann, and R. Marquart, in *High Temperature Superconductors*, edited by H. C. Freyhardt, R. Flückiger, and M. Peuckert (DGM-Informationsgesellschaft mbH, Oberursel, 1991), p. 895.
- ²²Ch. Heinzl, Th. Theilig, P. Ziemann, J. Hörschele, M. Fandel, T. Staneff, and S. Haidlinger, J. Alloys Compounds **195**, 173 (1993).
- ²³T. Wolf and A. Majhofer, Phys. Rev. B **47**, 5383 (1993).